OPTIMAL DESIGN OF THE HEATER OF A STIRLING ENGINE COUPLED WITH A FLUIDIZED BED COMBUSTOR

S. Lombardi*, K. Bizon, G. Continillo**, F.S. Marra*****
marra@irc.na.cnr.it
* Università degli Studi di Napoli Federico II - DIME, Napoli, Italy
** Università del Sannio, Dipartimento di Ingegneria, Benevento, Italy
** Istituto di Ricerche sulla Combustione - CNR, Napoli, Italy

Abstract
This work investigates the possibility of inserting the head of a Stirling engine, more specifically the elements of the hot side heat exchanger, in direct contact with the sand of a Fluidized Bed Combustor. This choice is suggested by the expected much larger heat exchange coefficients between the multiphase fluidized bed medium and the surface of the heat exchanger, as compared with a heat exchanger located in the stream of hot flue gases. Moreover, the mechanical action exerted by the fluidized solid particles is expected to avoid the fouling problem usually encountered for the presence of many impurities in exhaust gases of a biomass combustion process. A mathematical model, which couples a model of the fluidized bed with a model of the Stirling engine, is been developed and used to determine the optimal working conditions with a proper design sizing of the Stirling hot side heat exchanger.

Introduction

The idea of using heat generated by combustion as a source for a Stirling engine dates back to the early achievements of Stirling Engines (SE). The original idea is to place the hot head of the engine as much as possible in direct contact of the flame generated by combustion, identifying the flame with the region of highest temperature and therefore as that which favors thermal exchange between the hot combustion gases and the working fluid of the engine.
The problems that concern the use of biomass in combination with a Stirling engine are concentrated on the transfer heat from the combustion gases to the work fluid of the SE. The temperature must be high, to obtain acceptable specific power and efficiency, and the heat exchanger must be designed so that the problems of fouling are minimized [1]. When facing these problems, the adoption of fluidized bed combustion offers, at least in principle, several advantages:
- The typical temperatures of combustion in a fluidized bed are of about 850° C and, then are perfectly compatible with those required for optimal operation of the SE. For example, typical temperatures required for the supply of SE EG-1000 of Sunpower [2] range between 600 °C (873 K) to 950 °C, with the upper temperature limited by reasons of technological strength of materials;

- At these temperatures, emissions of nitrogen oxides are low, which is a clear benefit in terms of environmental issues;
- The coefficients of heat exchange between the fluidized bed and the surfaces of the heat exchangers immersed in it, are typically at least 10 times greater than those between a gas and the heat exchanger. This reduces the required surfaces, minimizing the footprint of the equipment, and/or to obtain a high flux at lower temperatures, minimizing the losses of heat dispersed in the fumes;
- The fluidized bed automatically exerts a cleaning action on the surfaces of the heat exchanger, thus maintaining the exchange coefficients stably over time, minimizing the need for maintenance.

Because of the high temperatures in the combustion chamber and the risk of fouling, it is not possible to use a Stirling engine designed for natural gas, since the narrow passages in the heat exchanger are rapidly blocked when operating with fuels derived from biomass. Actually, fouling in processes of combustion of the biomass mainly occurs during the cooling of the fumes.
In this work, a rigorous optimization approach is applied, to find the optimal configuration of the heat exchanger in terms of geometrical design parameters and confirm, at least theoretically, the advantage of this solution.

Fluidized bed combustor: CSTR model

The model of the FBC has been described in detail in a companion paper [3]. This work addresses the aspects of the model relevant to the coupling with the Stirling Engine model. The description starts from the definition of the control volume, hereinafter CV, identified by the surface that surrounds the volume of the fluidized bed, and interacts with the external environment in different ways, as shown schematically in Fig. 1. The main energy fluxes are, per unit time: the inlet energy carried by the fluidization air, $Q_{C,in}$; the solar energy coming from the collector, Q_{CSP}; the energy delivered to the SE, Q_{SE}; the outlet energy carried by the hot gases leaving the FB, sum of fluidization air and combustion gases, $Q_{C,out}$; the heat transferred by radiation from the FB surface, $Q_{R,out}$; the thermal power due to biomass combustion, S_F; the mechanical power required for fluidization, P_{fl}.
Under typical conditions of operation of a FB, the gas velocity is everywhere low, in the order of few meters per second. Also, the overpressure needed to fluidize the bed is relatively small. It is thus reasonable to neglect pressure variations in the bed and to assume that density variations are primarily due to changes in temperature (subsonic motion), resulting $\rho_g T = const$. The total energy variation in the control volume (CV) is approximated as:

$$\frac{d}{dt}E = \frac{d}{dt}\left(\rho_g T C_{pg} V_g\right) + \frac{d}{dt}\left(\rho_s C_{ps} V_s T\right)_s \approx \rho_s V_s C_{ps}\frac{dT}{dt} = m_s C_{ps}\frac{dT}{dt} \qquad (1)$$

leading to the following expression for the total energy balance in the FB:

$$\frac{dT}{dt} = \frac{1}{m_s C_{ps}} \left[Q_{C,in} + Q_{CSP} + Q_{F,in} - Q_{SE} - Q_{C,out} - Q_{R,out} + \Delta H_F - P_{fl} \right] \qquad (2)$$

Subscripts *g* and *s* refer to gas and solid phase, respectively; *in* refers to inlet conditions.

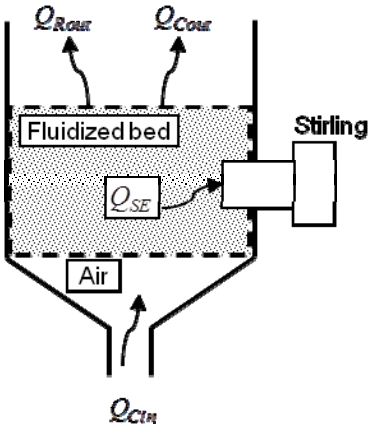

Figure 1. Control volume of the FBC and thermal fluxes

Stirling Engine: Bandurich-Normani model

The Stirling engine is modelled following Normani [4] who in turn followed Banduric [5]. The engine is considered partitioned in the following control volumes (Fig. 2): the compression space V_c; the expansion space V_e; the heater volume V_h; the cooler volume V_k; and the regenerator volume V_r. Cooler, heater and regenerator volumes form together the dead volume V_d.

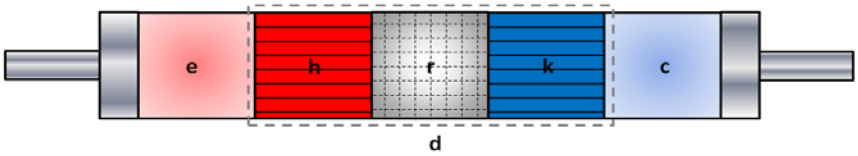

Figure 2. Control volumes of the Stirling engine model.

The mathematical model is based upon the following assumptions:

- the system is closed (there is no fluid leakage);
- the working fluid is considered ideal;
- effects of inertia of the working fluid are negligible;
- the dead space is isothermal;
- pressure in the dead space is uniform;
- compression and expansion spaces are adiabatic;
- the volumes of the compression and expansion spaces vary in time with

sinusoidal law;
- wall temperatures of heater and cooler are uniform and constant;
- gas temperatures in the heater and in the cooler are constant and equal to the temperature of heater and of the cooler, respectively;
- 80% of total pressure drop occurs inside the regenerator [3].

By writing the laws of conservation of mass and energy for each control volume, and applying appropriate mathematical manipulation, the whole system of equations assume the form reported in Table 1 .

Table 1. Model equations of the Stirling engine.

Differential equations

$$\begin{cases} \dfrac{dp_c}{dt} = -\gamma \dfrac{p_c}{V_c}\dfrac{dV_c}{dt} + \dfrac{dm_c}{dt}\dfrac{R\gamma T_{ck}}{V_c} \\ \dfrac{dp_e}{dt} = -\gamma \dfrac{p_e}{V_e}\dfrac{dV_e}{dt} + \dfrac{dm_e}{dt}\dfrac{R\gamma T_{eh}}{V_e} \\ \dfrac{dp_d}{dt} = -\dfrac{RT_d}{V_d}\left(\dfrac{dm_e}{dt} + \dfrac{dm_c}{dt}\right) \\ \dfrac{dm_c}{dt} = K_{Dc}\left(p_d - p_c\right)^{n_{dc}} \\ \dfrac{dm_e}{dt} = K_{De}\left(p_d - p_e\right)^{n_{de}} \end{cases}$$

Algebraic equations

$$\begin{cases} T_d = \dfrac{V_d}{\dfrac{V_h}{T_h} + \dfrac{V_k}{T_k} + \dfrac{V_{reg}}{T_{reg}}} \\ T_{reg} = \dfrac{\left(1-\varepsilon_1\right)T_h - \left(1+\varepsilon_2\right)T_k}{\ln\left(\dfrac{\left(1-\varepsilon_1\right)T_h}{\left(1+\varepsilon_2\right)T_k}\right)} \\ V_d = V_h + V_k + V_r \\ T_{ck} = T_c + 1/2\left(1 + \dfrac{dm_c/dt}{\left|dm_c/dt\right|}\right)\left(T_k - T_c\right) \\ T_{eh} = T_e + 1/2\left(1 + \dfrac{dm_e/dt}{\left|dm_e/dt\right|}\right)\left(T_h - T_e\right) \\ pV = mRT \end{cases}$$

The values n_{de} and n_{dc} are both fixed to 5/9 by Normani [4] and to 1/1.75 by Bandurich [5]. Here, the value 5/9 is adopted. The transport coefficients K_{de} and K_{dc} depend on various parameters, i.e. engine speed, geometric parameters of the heat exchangers of the heater and cooler (number of tubes, average length of the tubes, average diameter of the tubes), type of the working fluid (air, hydrogen, helium). The calculation procedure of K_{de} and K_{dc} is reported in [3]. The thermal power absorbed is obviously given by $\dot{Q}_h = f \cdot Q_h$, where f is the operating frequency of the engine, and Q_h is the heat absorbed per cycle, given by the area under the expansion curve in the $p-V$ plane. The shaft power is given by:

$$\dot{W} = fW = f\left[\oint p_c dV_c + \oint p_e dV_e\right] \tag{3}$$

Finally, the efficiency of the Stirling engine is given by $\eta = \dot{Q}_h / \dot{W} = Q_h / W$.
Both the CSTR and Stirling Engine models have been coded in Matlab. The coupled model is obtained by equating the heat absorbed per cycle by the Stirling Engine with the corresponding heat flux in the CSTR model.

Design optimization
The Paretian multi-objective optimization approach is adopted [9], to conduct a search of all non-dominated compromise solutions, called also efficient solutions, in the space of the decision variables. A solution is said to dominate another solution if the former is better than the latter with respect to one objective function, without worsening all the other objectives. On the other hand, two solution are called indifferent if the first is better than the second for some objectives, while the second is better than the first in all other objectives. Let us define an objective space $Y \subseteq \mathbf{R}^{n_f}$. Then, a point $y \in Y$ is said to be Pareto optimal if no point $\tilde{y} \in Y$ exists such that $F^{-1}(\tilde{y})$ dominates $F^{-1}(y)$. A set of solutions

$$\Phi = \left\{ y \in Y \middle| y \text{ is Pareto optimal} \right\}$$

is called Pareto front, while $\Xi = \left\{ x \in X \middle| F(x) \in \Phi \right\}$ is called Pareto set. The sets Φ and Ξ characterize the solution of the multi-objective problem. This problem is solved using the software tool modeFRONTIER [10]. Except for a set of proprietary algorithms implemented in the platform, it features an open character which permits integration with other commercial (e.g. Matlab, Excel) and non-commercial software.

Results and conclusions
The design of the heat exchanger of the heater has been conducted in such a way as to maximize both mechanical power and global efficiency upon appropriate geometric and operational constraints. The decision variables considered are the geometrical parameters of the heat exchanger of the heater (number, diameter and average length of the tubes) and operating parameters (fuel mass flow rate, engine speed). Figure 4 reports the result of the optimization procedure aiming at maximizing both the mechanical power produced by the Stirling and the global efficiency. It emerges that the proposed system is able to yield a significant output, even for such a small system size, and with a small rate of fuel consumption, making this system adequate for household installations. Moreover, the results have shown that the heater placed inside the fluidized bed leads to better performance than with a classic gas-gas heat exchanger. By increasing fuel consumption, the bed temperature increases – but so do heat losses from the system, leading to an overall decrease of the effective power. It is worth noting that optimal points correspond to parameter values that can be achieved only with the Stirling heat exchanger configuration submerged in the fluidized bed. Results indicate that a more compact engine head is able to greatly enhance the global

efficiency as it favours a decrease of the losses in the dead space of the Stirling, while the heat flux is not affected, thanks to the enhanced heat transfer coefficient typical of bodies immersed in a fluidized bed.

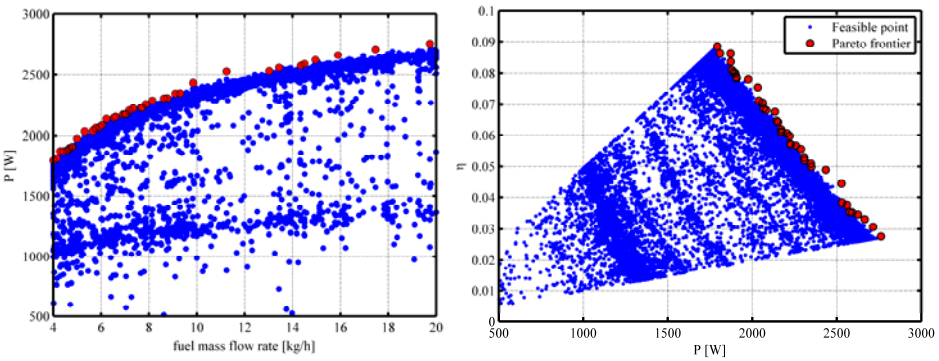

Figure 4. Mechanical power vs. fuel flow rate on the left; Solutions in the objective space (Mechanical Power, Global efficiency) on the right.

Acknowledgments

This project is partly supported by the Italian Ministry for the environmental, territory and sea protection (MATTM) under contract named MEGARIS.

References

[1] Vos, J. *Biomass energy for heating and hot water supply in Belarus*, Contract Report (BYE/03/G31), BTG (2006).

[2] Kim, S. Y., J. Huth, and J. G. Wood. 2005. "Performance Characterization of Sunpower Free-Piston Stirling Engines." Proceedings of AIAA IECEC2005 conference.

[3] Angrisani G., Bizon K., Chirone R., Continillo G., Fusco G., Lombardi S., Marra F. S., Miccio F., Roselli C., Sasso M., Solimene R., Tariello F., Urciuolo M. *Development of a New Concept Hybrid Solar-Biomass Cogeneration System*, *CPOTE Conference*, accepted (2012).

[4] Normani, F. *Stirling engine manual*. (2009).

[5] Banduric, R.D. and Chen, N. C. J. *Nonlinear analysis of Stirling engine thermodynamics*. Oak Ridge National Laboratory, (1984).

[6] Chen, N. C. J. and Griffin, E. P. *Effects of pressure-drop correlations on Stirling engine predicted performance*. Oak Ridge National Laboratory, (1983).

[7] Incropera, F. P. and DeWitt, D. P. *Fundamentals of heat and mass transfer*. Fourth Edition, School of Mechanical Engineering, Purdue University, (1996).

[8] Pareto V., *Cours d'economie Politique*, Rouge, Lausanne, Switzerland, (1896).

[9] *http://www.esteco.com/*

10.4405/35proci2012.VII6